JOURNAL OF MATERIALS SCIENCE 14 (1979) 1850–1861

Brittle interface layers and the tensile strength of metal matrix-fibre composites

M. Kh. SHORSHOROV, L. M. USTINOV, A. M. ZIRLIN, V. I. OLEFIRENKO, L. V. VINOGRADOV
A. A. Baikov Institute of Metallurgy, USSR Academy of Sciences, Moscow, USSR

The influence of brittle layers on the ultimate tensile strength of metal matrix composites is discussed. An equation has been derived to calculate the first critical thickness of the layer. The brittle layers have two effects on the fracture of the fibre, one of which is the value of the local stress near the tip of the crack, situated at the fibre–layer interface. Methods have been developed for the theoretical calculation of the critical stress intensity factor, K_{IC}, of brittle materials. Experimental results with B–SiC fibres have shown that their tensile strength is reduced with increasing thickness of the SiC layer. The critical thickness of the layer, t_l^*, for B–SiC fibres is about 1.0 to 7.5 μm, which coincides well with the theoretical value of t_l^*.

1. Introduction

Currently there is considerable interest in the problem of the influence of the interface layer on the tensile strength of metal matrix–fibre composites. This problem has great practical significance because increasingly composites are being developed which have either protective deposits on the fibres or an interaction zone between matrix and fibres. The majority of experimental results shows that the tensile strength of composites decreases as the thickness of the layer increases. The present paper develops the latter approach in a more general sense.

2. The critical thickness of the brittle interface layer

Let us consider a simple model system as shown in Fig. 1, which represents a fibre and concentric interface layer. The interface between fibre and the layer has a strength of not less than the components of the model and is considered to be ideally smooth. The diameter of the fibre d_f is constant and the fibres are of unit length. Stress is applied along the axis of the fibre and parallel to it.

Weibull has shown [1] that the strength of brittle materials is affected by their volume according to the equation

$$\sigma_1/\sigma_2 = (V_2/V_1)^{1/\beta} \quad (1)$$

where σ_1 and σ_2 are the average tensile strengths of a brittle material, having volumes V_1 and V_2 respectively; β is a Weibull coefficient, which shows the strength distribution of the material. Experimental data have shown that the tensile strength of the brittle layer is increased by a decrease in its thickness. It is possible to transform Equation 1 into the form

$$\bar{\sigma}_{l1}/\bar{\sigma} = (F_{l2}/F_{l1})^{1/\beta_1} \quad (2)$$

where $\bar{\sigma}_{l1}$ and $\bar{\sigma}_{l2}$ are the average tensile strengths of brittle layers having cross-sectional areas of F_{l1} and F_{l2} respectively; β_1 is a Weibull coefficient of the tensile strength distribution of the layer.

As the thickness of the layer changes fracture occurs in one of three different ways. In the first, the failure strain of the layer ϵ_{ul} is less that that of the fibre ϵ_{uf}, which is considered as constant in this model. The layer fractures first and is followed by fracture of the fibre. In the second case, ϵ_{ul} is greater than ϵ_{uf}, therefore the fibre fractures first and is followed by fracture of the layer. Thirdly ϵ_{ul} equals ϵ_{uf} and fracture of the components occurs simultaneously, i.e.

$$\bar{\epsilon}_{uf} = \bar{\epsilon}_{ul} \quad (3)$$

0022–2461/79/081850–13 $03.30/0
© 1979 Chapman and Hall Ltd.

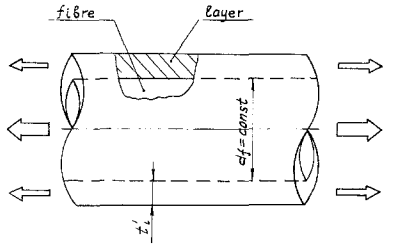

Figure 1 The model system – fibre/layer.

where $\bar{\epsilon}_{uf}$ and $\bar{\epsilon}_{ul}$ are the average failure strains of the fibre and the layer, respectively. Equation 3 is transformed into the following

$$\bar{\sigma}_{uf}/E_f = \bar{\sigma}_{ul}/E_l \qquad (4)$$

where E_f and E_l are the Young's moduli of the fibre and the layer respectively; $\bar{\sigma}_{uf}$ is the average tensile strength of the fibre; $\bar{\sigma}_{ul}$ is the average tensile strength of a layer of given thickness (we shall call this the critical thickness for the present). If we assume $\bar{\sigma}_{ul} = \sigma_{l1}$, $F_l = F_{l1}$, $F_l^* = F_{l2}$ and $\bar{\sigma}_{ul} = \bar{\sigma}_{l2}$ then Equations 2 and 4 will give the following equation

$$F_l^* = F_l \left(\frac{E_f \bar{\sigma}_{ul}}{E_l \bar{\sigma}_{uf}}\right)^{\beta_l}, \qquad (5)$$

where F^* is the critical cross-sectional area of the layer of critical thickness. It is more convenient to use another equation which is a modification of Equation 5. This equation has the following form

$$t_l^* = \left[\left(\frac{d_f}{2}\right)^2 + t_l(d_f + t_l)\left(\frac{E_f \bar{\sigma}_{ul}}{E_l \bar{\sigma}_{uf}}\right)^{\beta_l}\right]^{1/2} - \frac{d_f}{2} \qquad (6)$$

where t_l is the known value of the thickness of the layer for which $\bar{\sigma}_{ul}$ is known, t_l^* is the critical thickness of the layer, d_f is the diameter of the fibre. It is possible to simplify Equation 6, if we replace $\bar{\sigma}_{ul}$ by $\bar{\sigma}_{ul}^n$. Here $\bar{\sigma}_{ul}^n$ is the normalized value of the strength of the layer. The latter corresponds to the cross-sectional area of the layer, which is equal to the cross-sectional area of the fibre. Therefore, we have

$$t_l^* = \frac{d_f}{2}\left\{\sqrt{\left[1 + \left(\frac{E_f \bar{\sigma}_{ul}^n}{E_l \bar{\sigma}_{uf}}\right)^{\beta_l}\right]} - 1\right\}. \qquad (7)$$

$\bar{\sigma}_{ul}^n$ can be calculated from Equation 2. Equation 7 shows that t_l^* increases with the diameter of the fibre and the ratio $E_f\bar{\sigma}_{ul}^n/E_l\bar{\sigma}_{uf}$. In the latter case, t_l^* increases in parabolic fashion (Fig. 2). If

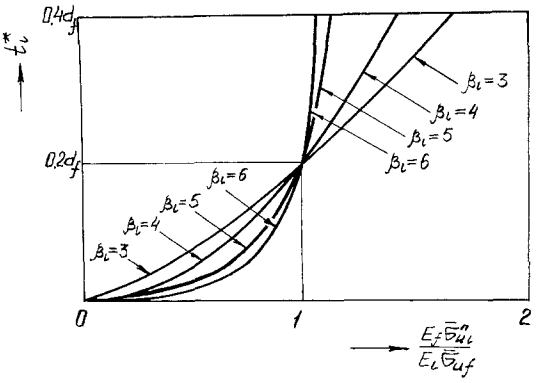

Figure 2 The graph showing effect of $E_f\bar{\sigma}_{ul}^n/(E_l\bar{\sigma}_{uf})$ on t_l^*.

$E_f\bar{\sigma}_{ul}^n/E_l\bar{\sigma}_{uf} = I$, then $t_l^* \cong 0.2\,d_f$. Therefore, from a practical view point it is desirable to select materials for fibres and protective layers in such a way that the ratio $E_f\bar{\sigma}_{ul}^n/E_l\bar{\sigma}_{uf}$ is as high as possible. If the ratio is less than unity, t_l^* will decrease with increasing β_l and vice versa (Fig. 2).

We now have an equation which enables us to calculate the critical thickness of the brittle interface layer for any composite material containing brittle fibres. If t_l/t_l^*, the layer will break first and only after that will the fibre break. Cracks which appear as a result of the fracture of the layer affect the fracture resistance of the fibre. They are, in fact, notches in the fibre. In the next section we shall show the interaction between these cracks and the fibre.

3. The influence of cracks in the layer on fibre fracture

Ustinov *et al.* [2] have studied the microstructural peculiarities of fractured layers in an aluminium/steel composite. Their experimental data have enabled them to construct a model of the propagation of cracks throughout the layer. According to this model (Fig. 3) the cracks appear at the layer–matrix interface (point S). The crack propagates through the layer towards the layer/fibre interface and eventually reaches the fibre (point C). If the stress intensity at point C is not enough to cause fracture of the fibre, the crack will by-pass the fibre completely. Otherwise the crack will enter the fibre and will propagate through the layer and the fibre simultaneously (Fig. 3). So in fact we have to discuss two different types of fracture. The first type (point C) is analogous to the fracture of a semi-infinite plate with an edge crack. The second type is analogous to the fracture of a bar with a circular crack.

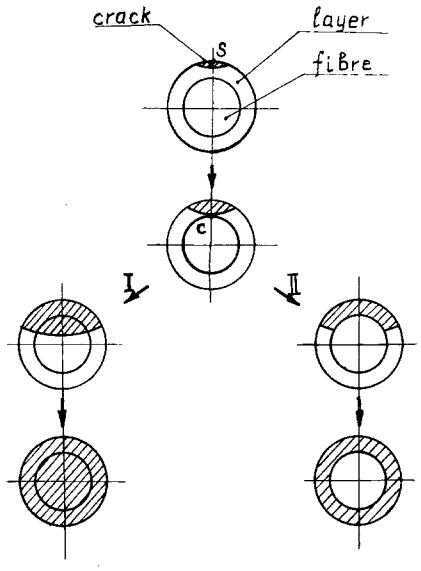

Figure 3 The model of crack propagation in the fibre/layer system.

Let us discuss the first case. This is represented by the model in Fig. 4. The model consists of a semi-infinite plate of two different brittle materials separated by the interface, which is parallel to the edge of the plate. The interface is strong enough to resist delamination. One component of the model, i.e. the layer, has only one finite dimension, that is, the thickness of the layer. This component contains the crack with its tip at the interface. At infinity the applied stresses are parallel to the interface and they have different values proportional to the Young's moduli of the components. This is a state of plane strain. Experimental data obtained by Ustinov *et al.* [2] permit us to regard the crack as quasi-static.

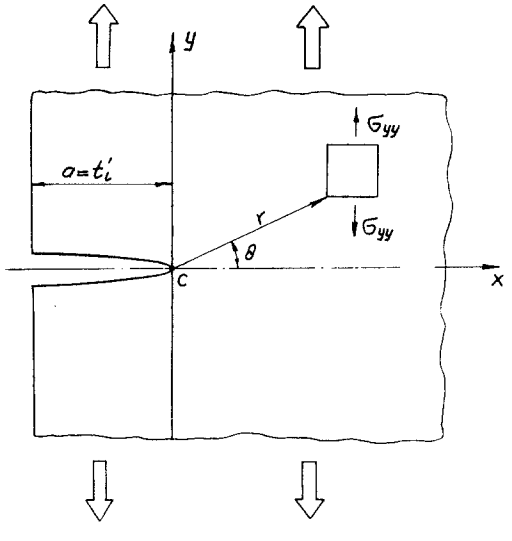

Figure 4 The first model of fracture of the fibre/layer system.

If the model system is homogeneous, i.e. the two components have similar properties, then the stress around point C (Fig. 4) will be given by the equations

$$\sigma_{xx} = \frac{K_I}{(2\pi r)^{1/2}} \cos\frac{\theta}{2}\left[1 - \sin\frac{\theta}{2}\sin\frac{3\theta}{2}\right] \quad (8a)$$

$$\sigma_{yy} = \frac{K_I}{(2\pi r)^{1/2}} \cos\frac{\theta}{2}\left[1 + \sin\frac{\theta}{2}\sin\frac{3\theta}{2}\right] \quad (8b)$$

$$\tau_{xy} = \frac{K_I}{(2\pi r)^{1/2}} \sin\frac{\theta}{2}\cos\frac{\theta}{2}\cos\frac{3\theta}{2}, \quad (8c)$$

where r is the distance from the tip of the crack (point C) to a given point, θ is the angle between the X-axis and the radius-vector r. We are more interested in stress σ_{yy} at a distance from point C of not more than approximately one atomic radius $r = r^*$. So if $\theta = 0$, Equations 8a to c become:

$$\sigma_{yy} = \frac{K_I}{(2\pi r^*)^{1/2}} \quad (9)$$

where K_I is the stress intensity factor. Paris and Sih [3] have shown that in case of a single phase model system, K_I is given by the equation

$$K_I = 1.12\sigma(\pi a)^{1/2} \quad (10)$$

where σ is the nominal stress, a is the greater semi-axis of the elliptical crack. If we come back to our model system which consists of two different materials, we must assume that K_I will be affected by the difference between the properties of these materials [4, 5]. Therefore, we will introduce the special factor κ, which is affected by the ratio E_l/E_f (see Appendix). So that we have

$$K_I = 1.12\kappa\sigma(\pi a)^{1/2}. \quad (11)$$

Equation 10 is valid for a fine fibre because the ratio d_f/t_l is more than $10 \div 100$. If we substitute in Equations 9 and 11 σ_f and t_l for σ and a, respectively, we obtain the following equation:

$$\sigma_{yy} = 0.79\kappa\sigma_f(t_l/r^*)^{1/2}, \quad (12)$$

where σ_f is the tensile stress in the fibre. We assume that $\sigma_f = \sigma_{uf}$, where σ_{uf} is the fracture stress of the fibre. Here the fracture of the fibre, which is initiated by the crack in the layer, occurs in practice simultaneously with the fracture of the

layer, i.e. at the fracture strain of the layer $\bar{\varepsilon}_{ul}$. Therefore, σ_{uf} is given by Equations 2 and 3 in the following way:

$$\frac{\bar{\sigma}_{uf}}{E_f} = \bar{\sigma}_{uf} = \bar{\sigma}_{ul} = \frac{\bar{\sigma}_{ul}}{E_l} = \frac{\bar{\sigma}_{11}}{E_l} = \frac{\bar{\sigma}_{12}}{E_l}\left(\frac{F_{12}}{F_{11}}\right)^{1/\beta_l}$$

and finally

$$\sigma_{uf} = \frac{E_f}{E_l}\bar{\sigma}_{12}\left(\frac{t_{12}}{t_{11}}\right)^{1/\beta_l}. \qquad (13)$$

After substituting t_l, t_{12} and σ_{12} by t_l', t_l and $\bar{\sigma}_{ul}$, respectively and inserting Equation 13 into Equation 12, we have the general equation

$$\sigma_{yy}^{I} = 0.79\kappa \frac{E_f}{E_4}\bar{\sigma}_{ul} t^{1/\beta_4}(t_l')^{1/2-1/\beta_l}. \qquad (14)$$

Here σ_{ul} and t_l are the known values of the strength and thickness of the layer, respectively, t_l' is the current value of the thickness of the layer. Equation 14 shows that σ_{yy}^{I} increases with t_l' (Fig. 5). If σ_{yy}^{I} is greater than $\sigma_{uf}^{t} \simeq E_f/10$ (σ_{uf}^{t} is the theoretical ultimate tensile strength of the fibre material), then the fracture of the layer will immediately initiate the fracture of the fibre at point C (Fig. 4).

Let us calculate σ_{yy}' for a number of well-known layer/fibre systems at condition $t_l^* = t_l'$ in order to ascertain whether or not the fracture of the layer immediately initiates the fracture of the fibre. First we must calculate the critical thickness of the layer t_l^*, using Equation 7, and then σ_{yy}^{I} using Equation 14. The results of these calculations are shown in Table I. The layer and the fibre will fracture simultaneously if $\sigma_{yy} \geqslant \sigma_{uf}^{t}$. Kelly [6] has shown that the factor β_l equals from 3 to 6. Table I shows that for the system B/(BN) where the ratio $E_f\bar{\sigma}_{ul}^{n}/\bar{\sigma}_{uf}E_l \geqslant 1$ in practice, there is no detrimental effect of a layer of any thickness on the strength of the fibres. For the three systems B/(B_4C), B/(SiC) and B/(BN), the fracture of a layer of critical thickness in practice always initiates immediate fracture of the fibre. Morin [7] has shown that in the system B/(B_4C), the strength of the fibre begins to decrease when the thickness of the layer is more than 7 to 8 μm. This more or less coincides with the calculated value of the critical thickness of the layer of B_4C when β_l equals 3 to 4. Camahort [8] and Ryder *et al.* [9] have shown that the tensile strength of the system B/(BN) did not decrease when the thickness of the layer was equal to $\sim$0.4 μm. Unfortunately, there are no further data for this sytem. Nevertheless the existing data do not contradict our calculated values for this system.

There are systems (two are shown in Table I – B/TiB_2 and B/AlB_2), where the fracture of the layer does not always immediately initiate fracture of the fibre. In this case the crack in the layer at the moment of meeting the fibre at point C (Fig. 3) creates σ_{yy}^{I}, which is less than σ_{uf}^{t}, thus the crack from the layer will not enter the fibre but will pass around it, as shown in Fig. 3. Therefore a new model should be discussed which comprises of a cylindrical fibre, a co-axial cylindrical layer and a circular notch (Fig. 6). The notch tip is situated on

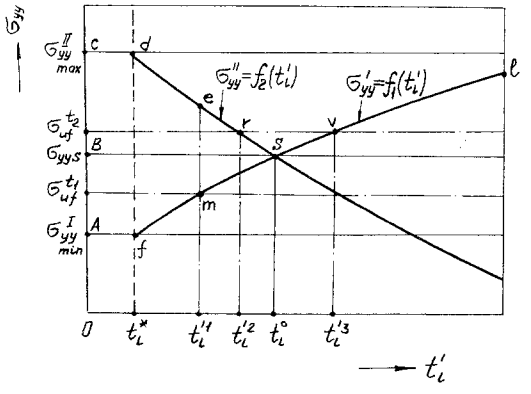

Figure 5 The effect of t_l' on σ_{yy}.

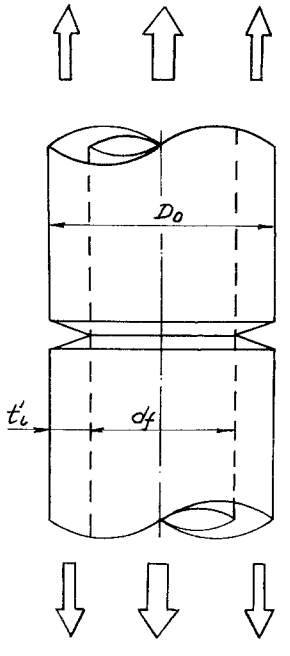

Figure 6 The second model of fracture of the fibre/layer system.

TABLE I The calculated characteristics of a number of fibre/layer systems

Fibre/ (deposit)	Fibre		Layer (deposit)			$t_{l_1}^{*}$ (μm)	Factor κ	σ_{uf}^{t}, (kg mm^{-2})	Stress σ_{yy}^{I}, (kg mm^{-2})	Will the fibre fracture due to σ_{yy}^{I}	Stress σ_{yy}^{II} (kg mm^{-2})	Will the fibre fracture due to σ_{yy}^{II}
	$E_f \times 10^{-3}$ (kg mm^{-2})	$\bar{\sigma}_{uf}$ (kg mm^{-2})	$E \times 10^{-3}$ (kg mm^{-2})	$\bar{\sigma}_{ul}^{n}$ (kg mm^{-2})	β_l							
B/(SiC)	38	350	47	230	3	3.62	1.11	3800	31 600	yes	–	–
	38	350	47	230	4	1.90	1.11	3800	23 400	yes	–	–
	38	350	47	230	5	1.04	1.11	3800	17 350	yes	–	–
	38	350	47	230	6	0.51	1.11	3800	12 400	yes	–	–
B/(B_4C)	38	350	47	230	3	3.62	1.11	3800	31 600	yes	–	–
	38	350	47	230	4	1.90	1.11	3800	23 400	yes	–	–
	38	350	47	230	5	1.04	1.11	3800	17 350	yes	–	–
	38	350	47	230	6	0.51	1.11	3800	12 400	yes	–	–
B/(BN)	38	350	9	140	3	70.6	0.48	3800	71 300	yes	–	–
	38	350	9	140	4	101.13	0.48	3800	86 700	yes	–	–
	38	350	9	140	5	141.97	0.48	3800	104 000	yes	–	–
	38	350	9	140	6	196.0	0.48	3800	123 600	yes	–	–
B/TiB_2	38	350	51	100	3	0.24	1.15	3800	8 330	yes	–	–
	38	350	51	100	4	0.05	1.15	3800	3 900	yes	–	–
	38	350	51	100	5	0.011	1.15	3800	1 840	no	31 400	yes
	38	350	51	100	6	0.002	1.15	3800	810	no	32 500	yes
B/AlB_2	38	350	42	70	3	0.145	1.05	3800	5 960	yes	–	–
	38	350	42	70	4	0.030	1.05	3800	2 670	no	27 600	yes
	38	350	42	70	5	0.005	1.05	3800	1 128	no	28 500	yes
	38	350	42	70	6	0.0008	1.05	3800	464	no	29 350	yes

the fibre/layer interface. The materials of the layer and the fibre are different and have different Young's moduli E_f and E_l and tensile strengths of $\bar{\sigma}_{uf}$ and $\bar{\sigma}_{ul}$. The model is loaded at infinity by stresses in the layer, σ_l, and the fibre, σ_f, which are proportional to the Young's moduli, E_l and E_f.

If this model (Fig. 6) was homogeneous, the stress intensity factor would be calculated according to Paris and Sih [3] from the equation

$$K_I = \sigma(\pi D_0)^{1/2} f(d_f/D_0), \qquad (15)$$

where σ is the nominal stress in the cross-sectional area $\pi d_f^2/4$ and factor $f(d_f/D_0)$ is a function of the ratio d_f/D_0. In composite materials, the ratio d_f/D_0 must not be less than 0.9, so $f(d_f/D_0) \simeq 0.2$. However, our model has two components of different materials, therefore K_I must be affected by the ratio E_f/E_l. We can depict this effect by introducing factor κ into Equation 15, giving

$$K = 0.2\kappa\sigma_f(\pi D_0)^{1/2} \qquad (16)$$

where σ_f is the nominal stress in the fibre. If we insert Equations 13 and 16 into Equation 9 and assume $t_{l1} = t_l'$, $t_{l2} = t_l$, $\bar{\sigma}_{l2} = \bar{\sigma}_{ul}$, $\sigma_f = \bar{\sigma}_{uf}$, then we shall have the equation for calculating σ_{yy}^{II} at the tip of the crack for the second model (Fig. 6).

$$\sigma_{yy}^{II} = 0.14\,\kappa(\bar{\sigma}_{ul}/E_l)E_f t^{1/\beta_l}(r^*)^{-1/2}(d_f + 2t_l')^{1/2}. \qquad (17)$$

It is also necessary to remember that σ_{yy}^{I} and σ_{yy}^{II} are stresses which appear during fracture of the layer. In fact, for both models, the layer fractures at the same fracture strain $\bar{\varepsilon}_{ul}$ (see Equation 3). Equation 17 shows that if $\beta_l = 3$ to 6 then σ_{yy}^{II} will decrease with increasing t_l', (Fig. 5). The curves of Equations 14 and 17 intersect each other at t_l', which equals t_l^0.

$$t_l^0 \simeq 0.034\,d_f \qquad (18)$$

Equation 18 was derived by assuming that $\kappa_1 \simeq \kappa_2$ (for the sake of simplicity). We can see that if $t_l' < t_l^0$, then $\sigma_{yy}^{II} > \sigma_{yy}^{I}$ (Fig. 5). Fig. 5 shows how σ_{yy} changes with changing of thickness of the layer. Let us look at Fig. 5 in detail. First it can be divided into four major areas from the viewpoint of the theoretical strength of the fibre, σ_{uf}^t.

Area OA. Here $\sigma_{uf}^t \leqslant \sigma_{yy\,min}^{I}$, where $\sigma_{yy\,min}^{I}$ is the minimum stress σ_{yy}^{I}. This can be calculated by inserting a value t^* in Equation 15. At $t_l' \geqslant t_l^*$ only the first model works (Fig. 4) and σ_{yy}^{I} changes from point f (at $t_l' = t_l^*$) to point L (Fig. 5). The

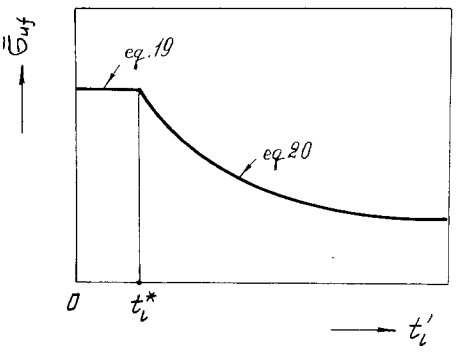

Figure 7 The effect of t_l' on $\bar{\sigma}_{uf}$ when $\sigma_{uf}^t \leqslant \sigma_{yys}$.

strength of the fibre $\bar{\sigma}_{uf}$ for this area is calculated from the equations:

$$\bar{\sigma}_{uf} = \text{const} = \bar{\sigma}_{uf}^{i} \quad \text{at } 0 \leqslant t_l' \leqslant t_l^* \qquad (19)$$

$$\bar{\sigma}_{uf} = (E_f/E_l)\bar{\sigma}_{ul}(t_l/t_l')^{1/\beta_l} \quad \text{at } t_l' \geqslant t_l^*, \qquad (20)$$

where $\bar{\sigma}_{uf}^{i}$ is the initial strength of the fibre (without layer). These equations give a curve, which shows change of the fibre strength σ_{uf} as a function of the thickness of the layer (Fig. 7). We can see that for the area OA, where $\sigma_{uf}^t \leqslant \sigma_{yy\,min}^{I}$, there is only one characteristic thickness, which we call the critical thickness t_l^*; the latter divides the graph in Fig. 7 into two parts. In the first part, where $0 \leqslant t_l' \leqslant t_l^*$, fracture of the model system is initiated by fracture of the fibre. In the second part, where $t_l' \geqslant t_l^*$, fracture of the model system is initiated by the fracture of the layer. Here σ_{uf} decreases monotonically with increasing t_l'.

Area AB. Here $\sigma_{yy\,min}^{I} < \sigma_{uf}^t \leqslant \sigma_{yys} \cdot \sigma_{yys}$ is calculated by inserting t_l^0 into Equation 14 or 17. The strength of the system is determined by Equation 19 (if $0 \leqslant t_l' \leqslant t_l^*$) and Equation 20 (if $t_l' \geqslant t_l^*$). Now let us discuss a specific example. We assume the fibre has the theoretical strength $\sigma_{uf}^t = \sigma_{uf}^{t1}$ (Fig. 5). We shall trace how σ_{yy} changes with increasing t_l'. If $0 \leqslant t_l' \leqslant t_l^*$, the fracture of the system will be initiated by the fracture of the fibre, so that the strength of the system is determined by Equation 19. If $t_l^* \leqslant t_l' < t_l^{II}$, then $\sigma_{yy}^{I} < \sigma_{uf}^t < \sigma_{yy}^{II}$. Therefore, the system fractures according to the second model (Fig. 6). Here σ_{yy}^{II} changes from point d (at $t_l' = t_l^*$) to point e (at $t_l' \approx t_l'^{I}$) (Fig. 5). If $t_l' \geqslant t_l'^{I}$ then $\sigma_{uf}^{t1} \leqslant \sigma_{yy}^{I}$; the system fractures according to the first model (Fig. 4) and σ_{yy}^{I} changes from point m to point L. In this example the fracture stress, σ_{yy}, changes along the curve demsL. If $\sigma_{uf}^{t'} = \sigma_{yys}$ then σ_{yy} will change along the curve desL. For the area AB a typical

graph $\bar{\sigma}_{uf}$ versus t_1' is the same as the analogous graph for the area OA (Fig. 7). Here again there is only one characteristic thickness of the layer, i.e. the first critical thickness t_1^*.

Area BC. Here $\sigma_{yys} < \sigma_{uf}^t \leqslant \sigma_{yy\,max}^{II} \cdot \sigma_{yy\,max}$ is calculated by inserting t_1^* into Equation 17. If $0 \leqslant t_1' \leqslant t_1^*$, the strength of the system will be determined by Equation 19, but if $t_1' \geqslant t_1^*$ and $\sigma_{uf}^t \leqslant \sigma_{yy}^{II}$ or $\sigma_{uf}^t \leqslant \sigma_{yy}^{I}$, it will be determined by Equation 20. However, in this area it is possible to meet a case where $\sigma_{yy}^{II} < \sigma_{uf}^t > \sigma_{yy}^{I}$, and then fracture of the layer does not immediately initiate fracture of the fibre. Therefore for the fracture of the fibre it is necessary to apply an additional load to the system until σ_{yy} reaches σ_{uf}^t. In this case the strength of the fibre is determined by the equation

$$\bar{\sigma}_{uf} = \frac{\sigma_{uf}^t (r^*)^{1/2}}{0.14\,\kappa (d_f + 2t_1')^{1/2}} . \qquad (21)$$

Equation 21 was derived from Equations 9, 13 and 15 and it is suitable for certain interval values of t_1'. This interval can be found by inserting σ_{uf}^t into Equations 14 and 17 and by their joint solution. A typical graph $\bar{\sigma}_{uf}$ versus t_1' for the area BC is shown in Fig. 8. Let us discuss another specific example. We assume that the fibre has a theoretical strength σ_{uf}^{t2} (Fig. 5). For the interval $t_1^* \leqslant t_1' \leqslant t_1'^2$ we have $\sigma_{yy}^{I} < \sigma_{uf}^{t2} \leqslant \sigma_{yy}^{II}$ and the system fractures according to the second model. For the interval $t_1'^2 < t_1' < t_1'^3$, $\sigma_{yy}^{II} < \sigma_{uf}^{t2} > \sigma_{yy}^{I}$ and the system again fractures according to the second model. But for interval $t_1'^3 \leqslant t_1'$, $\sigma_{yy}^{I} \geqslant \sigma_{uf}^{t2}$, and the system fractures according to the first model. Thus for this example the local fracture stress σ_{yy} must change along the line drvL and $t_1'^2 = t_1^{**}$, $t_1'^3 = t_1^{***}$ (Figs. 5 and 6).

The area above point C. Here $\sigma_{uf}^t > \sigma_{yy\,max}^{II}$.

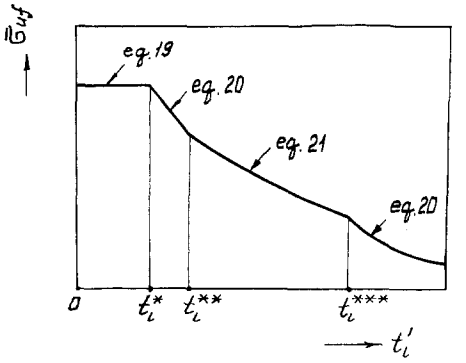

Figure 8 The effect of t_1' on $\bar{\sigma}_{uf}$ when $\sigma_{yys} < \sigma_{uf}^t < \sigma_{yy\,max}^{II}$.

If $0 \leqslant t_1' \leqslant t_1^*$, the strength of the fibre will be determined by Equation 19, but if $t_1' > t_1^*$, the strength of the fibre will be determined by Equation 21, because here $\sigma_{uf}^t > \sigma_{yy\,max}^{II} > \sigma_{yy}^{I}$. A typical graph of $\bar{\sigma}_{uf}$ versus t_1' for the area above point C is shown in Fig. 7.

The Fig. 5 shows that a situation is possible where the fracture of the layer does not immediately initiate fracture of the fibre. The graph $\bar{\sigma}_{uf}$–t_1' shown in Fig. 8 has four specific parts and three critical thicknesses of the layer; t_1^*, t_1^{**} and t_1^{***}. t_1^{**} and t_1^{***} can be calculated from equations

$$t_1^{**} = \left[\frac{E_1 (r^*)^{1/2}}{7.9\,\kappa \bar{\sigma}_{ul} t_1^{1/\beta_1}}\right]^{2\beta_1/(\beta_1 - 2)} \qquad (22)$$

$$t_1^{***} \approx d_1^{\beta_1/2} \left[1.4\,\kappa \frac{\bar{\sigma}_{ul}}{E_1} t_1^{1/\beta_1} (r^*)^{-1/2}\right]^{\beta_1} . \qquad (23)$$

The equation for calculating σ_{yys} can be derived from Equations 14 or 17 and 18, so that we have

$$\sigma_{yys} = 0.79\,\kappa \frac{E_f}{E_1} \bar{\sigma}_{ul} t_1^{1/\beta_1} (r^*)^{-1/2} (0.034\, d_f)^{1/2 - 1/\beta_1} . \qquad (24)$$

It can be seen that the interval between t_1^{**} and t_1^{***} increases with the ratio $E_1/\bar{\sigma}_{uf}$ (through factor κ). In principle, it is possible that the third critical thickness can be missing from the area BC.

Let us return to Table I. We can see that the systems B/(B_4C), B/(SiC) and B/(BN) are positioned in the area OA below point A in Fig. 5, but that systems B/TiB_2 and B/AlB_2 occur in the area AB above point A and below point S (if $\beta_1 = 4$ to 6). If $\beta_1 = 3$, these systems will be disposed in the area OA below point A, because in this case $\sigma_{uf}^t = E_f/10 = 3800\ \mathrm{kg\,mm^{-2}}$ which is less than $\sigma_{yy\,min}^{I}$. Nevertheless, all five systems have a similar plot of $\bar{\sigma}_f$ versus t′ which is shown in Fig. 7. However, systems B/(B_4C), B/(SiC) and B/(BN) fracture only according to the first model, and systems B/TiB_2 and B/AlB_2 fracture according to the first *and* second models: if $t_1' < t_1'^{I}$ (Fig. 5), they will fracture according to the first model. We have met this transition situation during calculation of σ_{yy} due to the fracture of the layer of the critical thickness. This is shown in the last four columns of Table I. When $\beta_4 = 3$, the systems B/TiB_2 and B/AlB_2 will only fracture according to the first Model (Table I and Fig. 7).

Table I shows for all the systems discussed that the fracture of the layer of any thickness t_1' ($t_1' \geqslant t_1^*$) immediately initiates the fracture of the fibre. However, Fig. 5 shows that, in principle, it is possible to meet systems where this does not always immediately occur.

4. Experimental study of the influence of the thickness of the layer (deposit) of SiC on the UTS of B–SiC fibres

For experimental verification of the theory, B–SiC fibres were used. Some early results have been published [10]. The diameter of the boron core was 0.1 mm, and the thicknesses of the SiC layers were 1.5, 3, 5 and 8.5 μm. The layers were produced by a gas chemical condensation process at a fixed temperature for all thicknesses. The thickness of the layer increased with the duration of the process. The temperature and duration of the process, however, were not so great as to reduce noticeably the strength of the boron fibre.

All fibres were tested on a "Shemadzu" tensile test machine with deformation rate of 0.1 sec^{-1}. The gauge length of the samples was 25 mm. The samples were prepared by a standard method, which is typical for these kinds of samples.

The results of this test are shown in Table II and in Fig. 9. They show that a drastic decrease in strength of the fibres will occur when the thickness of the layer is greater than 1.5 μm.

Fig. 9 shows the experimental and theoretical results for the tensile strength of the B–SiC fibres. The calculated results are shown by curves drawn for different values of β_1(β_1 = 4, 5 and 6). The results were calculated from the equation:

$$\bar{\sigma}_{u,\,B/SiC} = \bar{\sigma}_{u,\,SiC} V_{SiC} + \bar{\sigma}_{u,\,B} V_B \qquad (25)$$

where $\bar{\sigma}_{u,\,B/SiC}$, $\bar{\sigma}_{u,\,SiC}$ are the tensile strength of B–SiC and SiC fibres, respectively. $\bar{\sigma}_{u,\,SiC}$ was calculated from Equation 25 assuming that $\bar{\sigma}_{12}$ = 200 kg mm^{-2} when the thickness of the layer

TABLE II Tensile strength of the B/SiC fibres with different layer thicknesses

t_1'(μm)	$\bar{\sigma}_u$, B/SiC (kg mm^{-2})	$\bar{S}_u$, B/SiC, (kg mm^{-2})	Number of samples
0	298	48.3	63
1.5	290	58.5	52
3.0	247	50.6	52
5.0	233	18.5	64
8.5	165	12.9	67

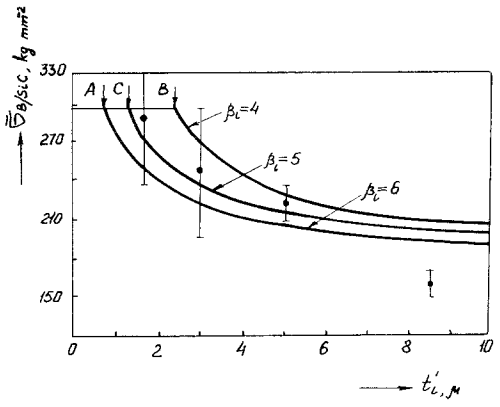

Figure 9 Experimental results of tensile testing of B–SiC fibres with different thicknesses of the SiC layers. The curves were calculated theoretically.

equals ~0.02 mm (this is equivalent to a fibre diameter of 0.1 mm). V_{SiC} is the volume fraction of SiC in B–SiC fibres ($V_{SiC} = F_{12}$); V_B is the volume fraction of boron in B–SiC fibres. $\bar{\sigma}_{u,B}$ is the nominal tensile fracture stress in the boron component of the B–SiC fibres. This is calculated from Equation 20. We also used the following characteristic data in our calculation: E_{SiC} = 47 000 kg mm^{-2}; E_B = 38 000 kg mm^{-2} and the tensile strength of boron fibres (without the SiC layer), = 298 kg mm^{-2} (see Table II). The critical thicknesses of the SiC layer, t_1^*, calculated from Equation 7, were 3.88; 2.15; 1.18 and 0.65 μm for β_1 = 3, 4, 5 and 6, respectively.

We can see that the experimental and theoretical data for β_1 = 4 to 5 coincide quite well. These values of β_1 were more typical for SiC fibres. Nevertheless, there is quite a large discrepancy between experimental and theoretical data at a thickness of 8.5 μm. Further study has shown that the tensile strength of the boron fibres is itself drastically reduced due to too long a deposition process of the SiC layer with a thickness of 8.5 μm. Annealed boron fibres had an ultimate tensile strength, $\sigma_{u,B}$, of 229 kg mm^{-2}. This, and probably the cracks which appeared in the layer due to stresses in the components, are the reasons for discrepancy. The theoretical critical thickness of the layer t_1^* lies between points B (for β_1 = 4) and C (for β_1 = 5) (see Fig. 9). It is more probable that t_1^* equals ~1 μm.

The general conclusion from these experimental data is that our theoretical treatment is confirmed by the experimental results from tests on B/SiC fibres.

5. Assessment method for K_{IC} of brittle fibres

Archangelskaya and Mileiko [11] have obtained an equation which allows us to calculate K_{IC} for fibre composite materials, if we know K_{IC} of the matrix and fibres. At the moment there is no way of determining K_{IC} of the fibres alone.

Previous sections of this paper give an opportunity to develop a theoretical method of assessment of K_{IC} of brittle fibres. Let us return to model 1 (see Fig. 4), which represents a brittle fibre and a brittle layer. A crack in the layer is, in fact, a notch on the fibre. We assume that: (1) the model under consideration has a layer thickness equal to the first critical thickness, t_1^*; (2) σ_{yy} equals $\sigma_{uf}^t = E_f/10$. This means that appearance of a crack in the layer of critical thickness immediately initiates fracture of the fibre, if $\sigma_{yy} = \sigma_{uf}^t$. In this case the nominal tensile stresss in the fibre must be equal to the tensile strength of the fibre, which has no layer, because t_1' is not more than t_1^*.

This situation can be met in real systems, which are analogous to the systems like B/TiB_2 and B/AlB_2, if their t_1^* values equal 0.0566 μm at $\beta_1 =$ 3.94 or 3.56, respectively. The situation can be expressed by an equation, which is analogous to Equation 12; but we must replace σ_f by $\bar{\sigma}_{uf}^i$, and σ_{yy} by σ_{uf}^t. Therefore, we have

$$\sigma_{uf}^t = 0.79\,\kappa\bar{\sigma}_{uf}^i(t_1^*/r^*)^{1/2}. \quad (26)$$

As we have shown, the stress intensity factor of model 1 is expressed by Equation 11. This equation can be used for the above case in the following way. We assume $K_I = K_{IC}$, if $\sigma = \bar{\sigma}_{uf}$ and $t_1^* = a$. Therefore, the following joint treatment of Equations 11 and 26 will give us the equation

$$K_{IC} \cong 2.5\,\sigma_{uf}^t r^{*1/2}. \quad (27)$$

We can transform Equation 27, if we insert $E_f/10$ instead of σ_{uf}^t to give:

$$K_{IC} \cong 0.25\,E_f r^{*1/2}. \quad (28)$$

Equation 28 shows that only the Young's modulus of the fibre has a strong effect on the critical stress intensity factor of the fibre. In this paper the effect of the structure of the fibre on K_{IC} is not discussed, thus Equation 28 shows a lower value of K_{IC} for the brittle fibres than would normally be the case.

TABLE III Calculated values of K_{IC} of some high-strength brittle fibres

Fibre	$E_f \times 10^{-3}$ (kg mm^{-2})	K_{IC} (kg mm$^{-3/2}$)
Al_2O_3	47	6.43
Carbon, type I	39	5.34
Carbon, type II	24	3.29
BN	9	1.23
B	38	5.20
SiC	47	6.43
TiB_2	51	6.98
B_4C	47	6.43

Table III shows the calculated values of K_{IC} for the majority of well-known high-strength brittle fibres. In our calculations we used $r^* = \text{const} = 3 \times 10^{-7}$ mm. In reality, the lattice dimension is slightly different for different fibre materials, but this is not important in our calculations because the latter must be considered to approximate for the present. It is interesting to note that Kelly [6] has shown that the available data for K_{IC} of bulk alumina and reactor graphite are 13 to 14 and 1.4 to 4.3, respectively.

6. Conclusions

It has been shown that the brittle layer in the fibre composite material reduces the ultimate tensile strength of latter, if the thickness of the layer is greater than the critical thickness. The derived equation for the calculation of the critical thickness of the layer shows that it is proportional to the diameter of the fibre and is affected by the ultimate tensile strength and Young's moduli of the fibre and the layer. Equations have been derived which show the effect of the layer's thickness on the ultimate tensile strength of the layer/fibre system.

An experimental study using B–SiC fibres has shown that the critical thickness of the layer $t_1^* =$ 1.0 to 1.5 μm. Experimental data coincide well with those calculated theoretically. On the basis of the theory, a method has been developed for the theoretical calculation of the critical stress intensity factor, K_{IC} of brittle fibres. Values of K_{IC} for different brittle fibres have been established.

Appendix

Calculation of K_I

Let us consider an infinite plate separated by an interface of two phases (Fig. A1), have no different Young's moduli E_1 and E_2. The first phase has a crack perpendicular to the interface. We assume that:

(1) the strength of the interface is ideal (there is no delamination in the interface);

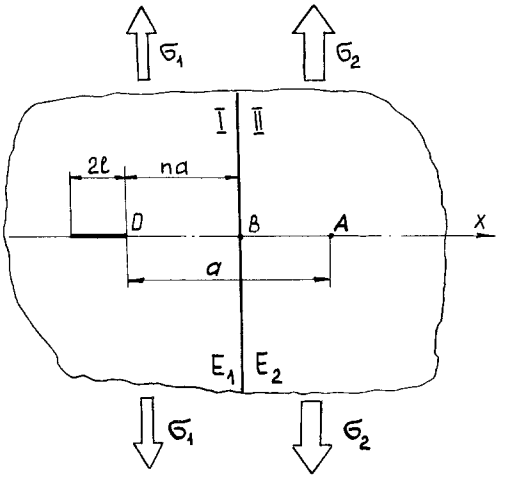

Figure A1 The model of a two-component infinite plate which has a crack to the left of the interface.

(2) the stress distribution at the tip of the crack is the same in a single phase plate, i.e.

$$\sigma(r;\theta) = [K_I/\sqrt{(2\pi r)}]\, f(\theta); \qquad \text{(A1)}$$

(3) the stress intensity factor, K_I changes drastically when the crack propagates through the interface;

(4) the load which is not sustained by half of the crack is compensated by a high local stress at the crack tip.

Now suppose that we section the crack along its length [12], discard one half of the plate and replace its effect by a system of equivalent forces. In this case the load which is not nearest to the interface half of the crack is balanced by the high local stress at the tip of the crack, i.e.

$$\int_0^a \sigma_{yy}(r;\theta)\, dr \qquad \theta = 0. \qquad \text{(A2)}$$

a defines the size of a zone of single stress and is calculated under the condition that $\sigma_{yy}(r;\theta)$ at $r = a$ is equal to nominal stress. Let us consider a case, when the crack is so close to the interface that a point a is in the second half of the plate. According to (3) above, we assume $\sigma_{yy}(r;\theta)$ changes by E_2/E_1 while the single stress propagates through the interface (Fig. A2). We can now write an equation for the conditions of balance:

$$\sigma_1 l - \int_0^a \sigma_{yy}(r;\theta)\, dr = \sigma_1 l - \int_0^b \sigma_{yy}(r;\theta)\, dr$$

$$-\int_b^a \frac{E_2}{E_1}\, \sigma_{yy}(r;\theta)\, dr = 0. \qquad \text{(A3)}$$

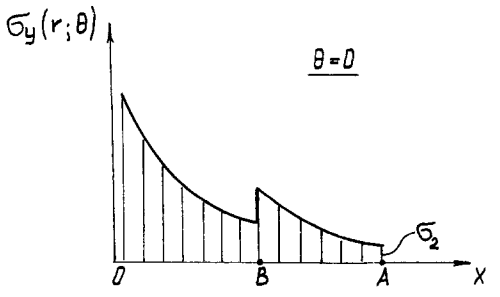

Figure A2 The peculiarity of the stress pole in the vicinity of the interface.

a is calculated from

$$\frac{E_2}{E_1}\, \sigma_{yy}(a;0) = \sigma_2. \qquad \text{(A4)}$$

Equations A1 and A4 give

$$\frac{E_2}{E_1}\, \frac{K_I}{\sqrt{(2\pi a)}} = \sigma_2.$$

According to the first assumption

$$\epsilon_1 = \epsilon_2$$

and

$$\sigma_1/E_1 = \sigma_2/E_2, \qquad \text{(A5)}$$

so we have

$$a = \frac{K_I^2}{2\pi\sigma_1^2}. \qquad \text{(A6)}$$

If we have $b = na$, where $0 \leqslant n \leqslant 1$, Equation A3 is transformed to become:

$$\sigma_1 l - \int_0^{an} \frac{K_I dr}{\sqrt{(2\pi r)}} - \int_{an}^a \frac{E_2 K_I dr}{E_1 \sqrt{(2\pi r)}} = 0. \qquad \text{(A7)}$$

After integration we have

$$K_I \sqrt{\left(\frac{2a}{\pi}\right)} \left[\frac{E_2}{E_1} + \sqrt{n}\left(1 - \frac{E_2}{E_1}\right)\right] = \sigma_1 l. \qquad \text{(A8)}$$

Equations A6 and A8 give us

$$K_I = \sigma_1 \sqrt{\left\{\frac{\pi l E_1}{E_2\,[1 + \sqrt{n}(E_1/E_2 - 1)]}\right\}}, \qquad \text{(A9)}$$

but Equations A5 and A9 give

$$K_I = \frac{E_1}{E_2}\, \sigma_2 \sqrt{\left\{\frac{\pi l E_1/E_2}{1 + \sqrt{n}\,[(E_1/E_2) - 1]}\right\}}. \qquad \text{(A10)}$$

From Equation A10, when the crack meets the interface, i.e. $\eta \to 0$, the stress intensity factor K_I equals:

$$K_I = \sigma_1 \sqrt{(\pi l E_1/E_2)}. \quad \text{(A11)}$$

When the crack is far from the interface, i.e. $n = 1$, we have

$$K_I = \sigma_1 \sqrt{(\pi l)}, \quad \text{(A12)}$$

Which is in agreement with K_I for a single-phase plate. The last result shows that if the crack is further from the interface than $\frac{1}{2}$, K_I may be calculated from the typical equation for a single-phase plate.

When $\eta \to 0$ and $E_1/E_2 < 1$, K_I decreases, and if $E_1/E_2 > 1$, K_I increases.

When the crack enters the second half of the plate (Fig. A3) K_I changes drastically. In this case, an equation of balance is:

$$\sigma_1 l(1-m) + \sigma_2 ml - \int_0^a \sigma_{yy}(r;\theta)\,dr = 0, \quad \text{(A13)}$$

where $0 \leqslant m \leqslant 1$. a is calculated from the equation:

$$a = \frac{K_I^2}{2\pi\sigma_2^2}. \quad \text{(A14)}$$

Integration of the Equations A5 and A13 give us

$$\frac{E_1}{E_2}\sigma_2(1-m)\,l + \sigma_2 ml = \frac{K_I^2}{\pi\sigma_2}, \quad \text{(A15)}$$

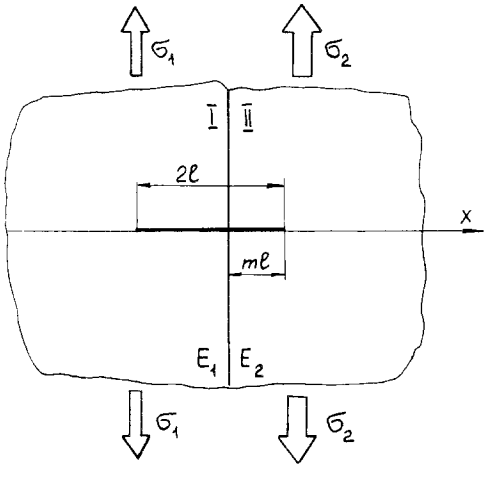

Figure A3 The model of a two-component infinite plate which has a crack to the right of the interface.

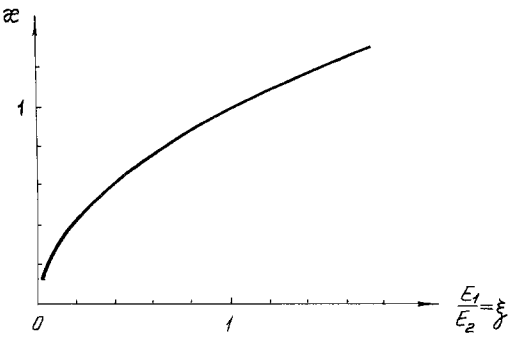

Figure A4 The effect of E_1/E_2 on κ.

therefore,

$$K_I = \sigma_2 \sqrt{\left\{\pi l \left[\frac{E_1}{E_2} + m\left(1 - \frac{E_1}{E_2}\right)\right]\right\}} \quad \text{(A16)}$$

If $m = 0$,

$$K_I = \sigma_2 \sqrt{\left(\pi l \frac{E_1}{E_2}\right)} \quad \text{(A17)}$$

and if $m = 1$,

$$K_I = \sigma_2 \sqrt{(\pi l)}. \quad \text{(A18)}$$

Equation A17 shows that if the crack enters the second half of the plate, K_I increases by E_1/E_2 and then decreases gradually until the value of K_I for a single-phase plate is reached. These results are in accordance with analogous results obtained by the finite element method [13, 14].

We now consider a semi-infinite plate of two different brittle materials, which was shown earlier in Fig. 4. The two phases are separated by the interface, which is parallel to one edge of the plate. One component of the model has only one finite dimension, apart from thickness. This component contains the crack. For this case it is necessary to make one change to assumption 4 which was adopted for the infinite plate. A particularly high local stress at the tip of the crack compensates only for load which is not along the whole length of the crack, σ_1 [21]. In accordance with this, it is necessary to substitute $2l$ for l in Equations A11 and A12. These equations give

$$K_I = \sigma_1 \sqrt{(2\pi E_1/E_2)} \quad \text{(A11a)}$$

$$K_I = \sigma_1 \sqrt{(2\pi l)}. \quad \text{(A12a)}$$

If we introduce the factor κ, which is affected by the ratio E_1/E_2, then we obtain the following equation from Equations A11a and A12a:

$$\sigma_1 \sqrt{(2\pi l E_1/E_2)} = \kappa\sigma_1 \sqrt{(2\pi l)}$$

and eventually

$$\kappa = \sqrt{(E_1/E_2)}. \qquad \text{(A19)}$$

If $E_1 = E_2$, then $\kappa = 1$. In Fig. A4 the effect of E_1/E_2 on κ is shown.

The same result, i.e. Equation A19, is achieved for the case of infinite plate which is shown in Fig. A1. This shows that the factor κ is not affected by the type of model system. Therefore, Equation A19 is valuable for a model of an infinite bar with a circular notch (Fig. 6).

References

1. W. WEIBULL, "A statistical theory of the strength of Materials", Ing. Vetenskaps. Acad. Hande (Roy. Swedish Inst. Eng. Research Proc.) No. 151 (1939).
2. L. M. USTINOV, V. I. ZHAMNOVA and M. Kh. SHORSHOROV, Proceedings of the fifth International Conference for Powder Metallurgy, Dresden, (1973) part II, p. 36–1.
3. P. C. PARIS and G. C. SIH, "Fracture Toughness Testing and its Application", ASTM Special Technical Publication, No. 381, (1964), p. 30.
4. A. R. ZAK and M. L. WILLIAMS. "Crack Point Stress Singularities at a Bimaterial Interface", GALCIT SM 42–I (1962) Californian Institute of Technology.
5. S. G. PAPAIOANNOU, P. HILTON and R. A. LUCAS, *Eng. Fract. Mech.* **6** (1974) 807.
6. A. KELLY. "Strong Solids" (Clarendon Press, Oxford, 1973).
7. D. MORIN, *Verre Textile Plast. Reinforc.* **3** (1974) 16.
8. J. L. CAMAHORT, *J. Comp. Mater.* **2** (1968) 104.
9. C. G. RYDER, A. E. VIDOZ, F. W. CROSSMAN and J. L. CAMAHORT, *ibid* **4** (1970) 264.
10. M. Kh. SHORSHOROV, A. M. ZIRLIN, L. M. USTINOV, L. V. KATINOVA, V. I. ZHAMNOVA, A. S. MITKIN and L. N. MOGUCHIJ, *Phisika i Himia obrabotki materialov (USSR)* (1976) 119.
11. I. N. ARCHANGELSKA and S. T. MILEIKO, *J. Mater. Sci.* **11** (1976) 356.
12. V. Z. PARTON and E. M. MOROZOV. "Mechanic of Elastic-plastic fracture" (Nauka, Moscow, 1974).
13. T. S. COOK and F. ERDOGAN, *Int. J. Eng. Sci.* **10** (1972) 677.
14. F. ERDOGAN, *Eng. Fract. Mech.* **4** (1972) 811.

Received 8 March and accepted 20 July 1978.